Standardised uptake values of 2-deoxy-2-[^{18}F]fluoro-D-glucose using PET/CT in normal cats

Y.K. Cho[1], K.C. Lee[2]

[1]Department of Radiological Technology, Daegu Health College, Daegu, Korea
[2]College of Veterinary Medicine, Chonbuk National University, Korea

ABSTRACT: In this study we assessed the normal physiological and dynamic thoracoabdominal distribution of ^{18}F fluorodeoxyglucose (^{18}F-FDG) uptake and the standardized uptake values (SUVs) of the major parenchymal organs in five normal young adult domestic short haired cats. Dynamic PET data were acquired with a transaxial field-of-view (FOV) PET/CT scanner, Regions of interests (ROIs) were manually drawn over the left ventricular free wall, left ventricular blood pool, liver, spleen, and left and right renal cortices. The SUVs of these organs were calculated for 5-min frames over the 90 min acquisition. The uptake of ^{18}F-FDG within the major organs, showed a tendency to gradually decline, except for the left ventricle and blood pool. The decrease in SUV was rapid after injection with a plateau occurring after 30 minutes. The uptake of ^{18}F -FDG within the hepatic parenchyma was low compared to that in the kidney at the beginning of study. A steady decline in the hepatic parenchyma SUV was quite similar to that observed for the kidneys .The SUV of ^{18}F-FDG within the spleen was low. Uptake of ^{18}F-FDG within the myocardium was minimal. These SUV data from the parenchymal organs of normal cats compares favourably with those of normal humans and dogs and can be used in feline studies using PET/CT for the evaluation of various diseases. Furthermore, PET/CT can provide higher quality images over shorter examination times than conventional PET.

Keywords: standardised uptake value (SUV), ^{18}F-FDG, cat, PET/CT

List of abbreviations:

^{18}F-FDG = 2-deoxy-2-[^{18}F]fluoro-D-glucose, **PET/CT** = positron emission tomography/computed tomography, **SUV** = standardised uptake value

The positron emission tomography/computed tomography (PET/CT) scanner, in which PET and CT are combined, represents an important development in the fields of disease phase diagnosis and oncology. This scanner shows high accuracy as the morphologic image and metabolism-functional inspection PET are confused (Gorospe et al. 2006; Tsukamoto and Ochi 2006).

In the oncology field, the clinical use of PET scan is frequent, and the image of distributed ^{18}F-FDG is used.

^{18}F-FDG, a glucose analogue, enters cells with the aid of the glucose transporter proteins GLUT-1 through GLUT-6, and is then phosphorylated (Fowler and Ido 2002).

A large number of malignant tumours exhibit a high number of specialised membrane transport proteins, and have a greater affinity for glucose than normal cells, thus resulting in an increased glucose flow into cancer cells. Thus, the accumulation of ^{18}F-FDG is greater in tumours than in normal cells.

The intake of ^{18}F-FDG depends on the supply of blood, the distributed quantity as well as the normal physiological intake of the tumour, and on the competitive intake course in other organs. Furthermore, ^{18}F-FDG intake by tumour tissues and surrounding healthy tissues depends on the time elapsed after injection (Visser et al. 2008).

The ^{18}F-FDG SUVs of feline heart muscle, liver and large intestine using PET are already known (LeBlanc et al. 2009).

This experiment, however, aimed to elucidate various other SUVs in the cat and to obtain dynamic

data using PET/CT, which is improved to allow the obtaining of a more accurate location. Combining PET with CT can more accurately depict the region of interest (ROI), thus resulting in an improved SUV.

Up to now, most PET studies have implemented total body scans. In the selected case, semi-quantitative analysis was implemented, and is based on the calculation of SUVs. These SUVs have become a universal measurement factor that indicates the glucose intake level within organs (Hamberg et al. 1994; Nuutinen et al. 1999; Liu et al. 2001; Abouzied et al. 2005).

This study was carried out to evaluate the importance of dynamic PET/CT in the study of malignant disease with regard to tumour diagnosis and the establishment of appropriate treatment plans. An additional goal of this study was to increase the reliability of SUVs of PET/CT inspection.

In a previous study by our group, only the static data from PET using a cat subject was obtained (LeBlanc et al. 2009). In comparison, the acquisition of dynamic data is more important than that of the static image as it gives important information regarding tracer distribution in time and space. The normal cat intake data is important for appropriate interpretation of ^{18}F-FDG PET/CT scans in clinical situations.

The physiological distributions of malignant tumours and normal tracer may cause confusion in positive pathological settings and with malignant tumours due to physiological diversity (Abouzied et al. 2005; Gorospe et al. 2006; Tsukamoto and Ochi 2006).

An additional limitation to the previous PET experiment by our group was that the subject was imaged in several positions using a micro PET scanner with a small field of view (7.8 cm) (LeBlanc et al. 2009).

In the present study, we addressed that limitation by using a scanner with a large field of view (16.2 cm), so we could obtain dynamic data in only one position.

The main purposes of this study were to determine the SUV, the normal physiological distribution of dynamic thoracoabdominal ^{18}F-FDG in normal cat organs, and to establish an image protocol for PET/CT using a large field-of-view(FOV) scanner for the investigation of tumour size and for optimisation of treatment plans (Tsukamoto and Ochi 2006; Macapinlac 2008).

MATERIAL AND METHODS

Five young adult domestic short haired cats weighing 3.0 ± 0.5 kg (mean ± SD) and ranging in age from 1–2 years (mean ± SD, 1.4 ± 0.5 years) were supplied by the laboratory animal facilities at the Veterinary Medicine Clinic of Chonbuk University. The cats were housed in facilities approved by the Office of Laboratory Animal Care at Chonbuk University.

Physical examinations, thoracoabdominal radiography, laboratory testing, and abdominal ultrasound examinations were performed on the animals.

The five cats were fasted for 24 h, and were premedicated with atropine (0.10 mg *i.m.*). Anaesthesia was maintained with zoletil (tiletamine + zolazepam) throughout the procedure.

The cats were placed in dorsal recumbency, and positioned within the PET/CT scanner gantry, so
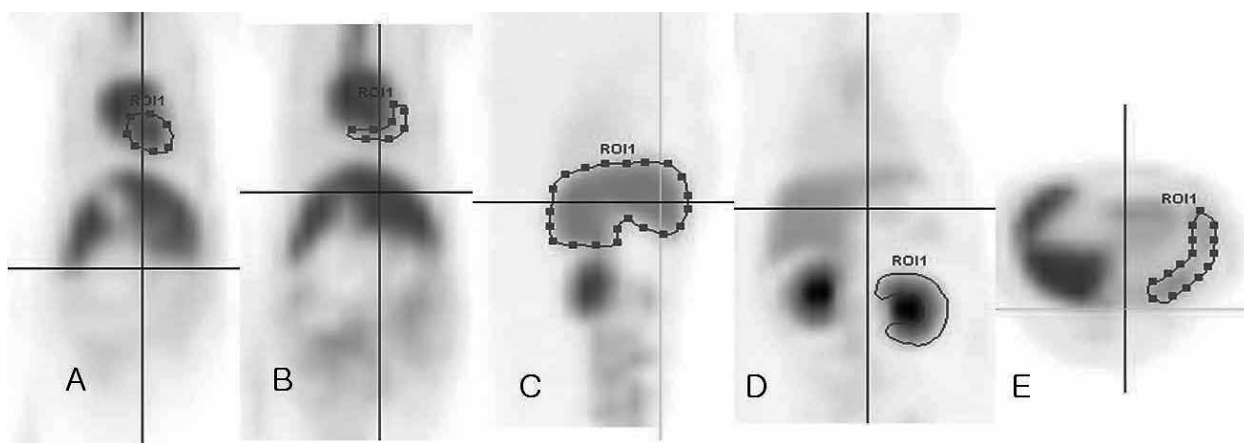

Figure 1. Depiction of representative regions of interest (ROI) manually drawn for image analysis and calculation of standardised uptake values over a 90 min time period for the thoracic and abdominal organs of five normal cats (A) blood pool ROI in the frontal plane, (B) myocardial ROI, (C) hepatic ROI in the sagittal plane, (D) renal cortical ROI in the frontal plane, (E) splenic ROI in the transverse plane

that the entire thorax and abdomen were included within the FOV.

A large FOV, cerium–doped lutetium oxyorthosilicate (LSO:Ce) PET/CT scanner is able to image low levels of radioactivity. Five large panels with an axial dimension of 16.2 cm and a transaxial dimension of 60.5 cm incorporating a total of 24 336. 4 mm × 4 mm × 20 mm LSO crystal elements providing a sensitivity of 4.4 cps/kBq were used. A fast LSO crystal for each point source served as a reference detector during the transmission coincidence acquisition (Liu et al. 2001). Two hundred and forty-eight 160 × 160, 3 mm-thick transaxial parallel slices were generated.

After deciding on the scan length, the CT scan (slice thickness 0.5 mm, scan time 25 s) was implemented, and dynamic PET (scan time: 90 min) was implemented by list mode.

The mean plasma glucose concentration before ^{18}F-FDG injection was 105 ± 20 mg/dl. The cats were injected intravenously with 25.9 ± 3.7 MBq (0.7 ± 0.1 mCi) of human-grade ^{18}F-FDG and a 90 min, dynamic list-mode acquisition was initiated simultaneously with the injection.

The ^{18}F-FDG uptake was evaluated at the ROI on the target organs or the uptake sites. The ROIs were manually drawn over the left ventricular free wall, left ventricular blood pool, liver, spleen, and finally, the left and right renal cortices (Figure 1). Particular caution was taken to exclude imaging of renal pelvic uptake due to accumulation of ^{18}F-FDG for urinary excretion.

The SUV was defined as the average decay-corrected tissue concentration of ^{18}F-FDG, in the region delineated by the ROIs divided by the radioactivity injected per kilogram of body weight (LeBlanc el al. 2008).

RESULTS

In Table 1, each organ shows a high SUV with intravenous injection; however, our data show a gradual decrease with time. The images of the chest and abdomen showed accumulation in most of the small and large intestines except for the lung where only low accumulation was observed.

Table 1. Serial mean standardised uptake values (SUVs) and standard deviations (SD) for the major organs of five normal cats imaged with ^{18}F-FDG PET/CT

| Time(s)	Right kidney		Left kidney		Spleen		Liver		Blood pool		Left ventricle	
	SUV	SD	SUV	SD	SUV	SD	SUV	SD	SUV	SD	SUV	SD
0	5.27	0.74	4.58	0.49	0.95	0.83	2.86	0.62	3.61	0.66	1.64	0.22
300	4.54	0.61	3.90	0.48	0.74	0.65	2.46	0.50	2.90	0.58	1.44	0.22
600	3.79	0.46	3.31	0.47	0.57	0.50	1.97	0.23	2.44	0.46	1.32	0.25
900	3.33	0.44	3.09	0.11	0.46	0.40	1.79	0.36	2.33	0.34	1.26	0.29
1200	3.02	0.38	2.88	0.15	0.41	0.36	1.67	0.36	2.15	0.33	1.29	0.31
1500	2.83	0.37	2.77	0.15	0.34	0.30	1.64	0.29	2.11	0.35	1.31	0.35
1800	2.65	0.25	2.63	0.13	0.32	0.28	1.45	0.29	2.13	0.36	1.34	0.40
2100	2.57	0.28	2.28	0.30	0.29	0.25	1.36	0.27	2.17	0.42	1.38	0.48
2400	2.42	0.27	2.20	0.27	0.24	0.22	1.32	0.27	2.16	0.50	1.40	0.58
2700	2.37	0.23	2.16	0.21	0.24	0.21	1.26	0.26	2.16	0.54	1.42	0.69
3000	2.28	0.17	2.10	0.22	0.22	0.20	1.16	0.26	2.08	0.73	1.44	0.83
3300	2.16	0.15	2.07	0.30	0.23	0.21	1.07	0.24	2.10	0.81	1.45	0.90
3600	2.04	0.21	2.00	0.34	0.24	0.21	1.00	0.20	2.05	0.86	1.46	0.96
3900	1.93	0.29	1.96	0.36	0.19	0.17	0.98	0.22	2.04	0.88	1.49	1.02
4200	1.89	0.23	1.93	0.37	0.19	0.17	0.94	0.22	2.01	0.93	1.53	1.10
4500	1.88	0.22	1.93	0.37	0.18	0.15	0.87	0.23	1.97	0.98	1.54	1.16
4800	1.85	0.25	1.87	0.32	0.17	0.15	0.85	0.23	2.00	1.01	1.57	1.22
5100	1.77	0.29	1.82	0.32	0.17	0.14	0.94	0.22	2.03	1.09	1.61	1.27
5400	1.69	0.29	1.78	0.32	0.17	0.14	0.78	0.14	2.11	1.23	1.67	1.37
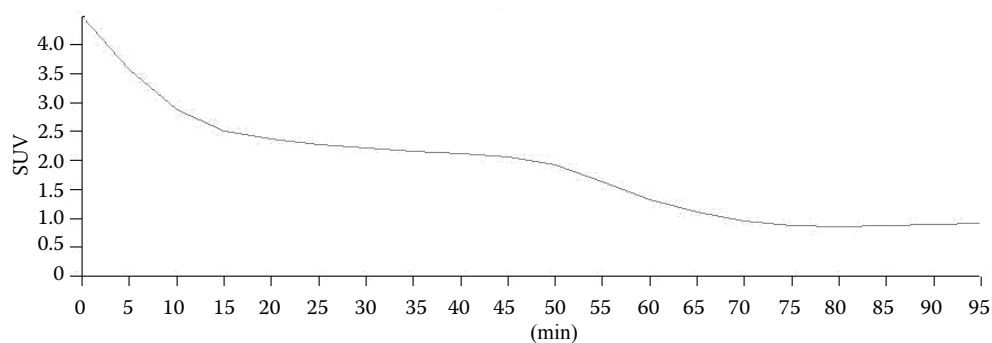
Figure 2. The time activity curve of ^{18}F-FDG obtained from the region of interest (ROI) around the blood pool of a cat
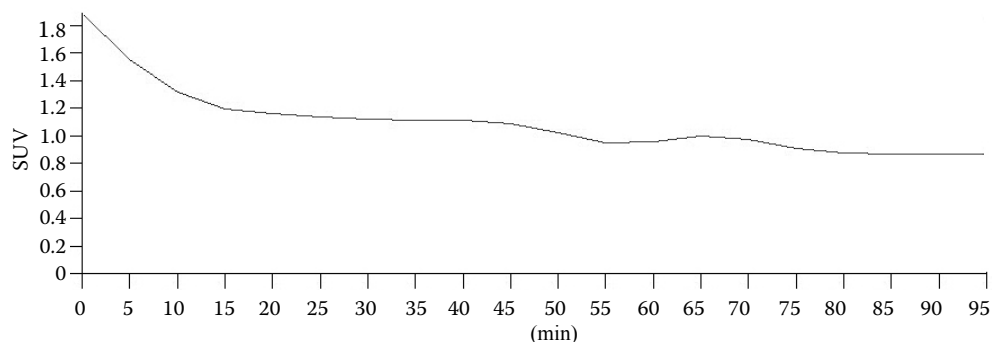

Figure 3. The time activity curve of ^{18}F-FDG obtained from the region of interest (ROI) around the left ventricle of a cat

High SUV values in the left and right kidneys, gathered fast to the bladder for excretion to the pelvis of the kidney and the ureter was observed in all images by 90 min.

The uptake of ^{18}F-FDG within both renal cortices was high at the beginning of acquisition (right kidney: SUV 5.27 ± 0.74, left kidney SUV 4.58 ± 0.49), and those values represented the highest levels observed among the organs examined over all time points.

The decrease in SUV was rapid after injection with a plateau occurring after 30 min (right kidney: 30 min SUV 2.65 ± 0.25, 60 min SUV 2.04 ± 0.21,

90 min SUV 1.69 ± 0.29; left kidney: 30 min SUV 2.63 ± 0.13; 60 min SUV 2.008 ± 0.34, 90 min SUV 1.78 ± 0.32) (Figure 2 and 3).

The uptake of ^{18}F-FDG within the hepatic parenchyma was low at the beginning of acquisition (SUV 2.86 ± 0.62) compared to that in the kidneys.

The steady decline in SUV observed in the hepatic parenchyma was quite similar to that observed in the kidneys (30 min SUV 1.45 ± 0.29, 60 min SUV 1.00 ± 0.20, 90 min SUV 0.78 ± 0.14) (Figure 4).

The SUV of ^{18}F-FDG in the spleen was relatively low (injection SUV 1.54 ± 0.83, 30 min SUV 1.04 ±
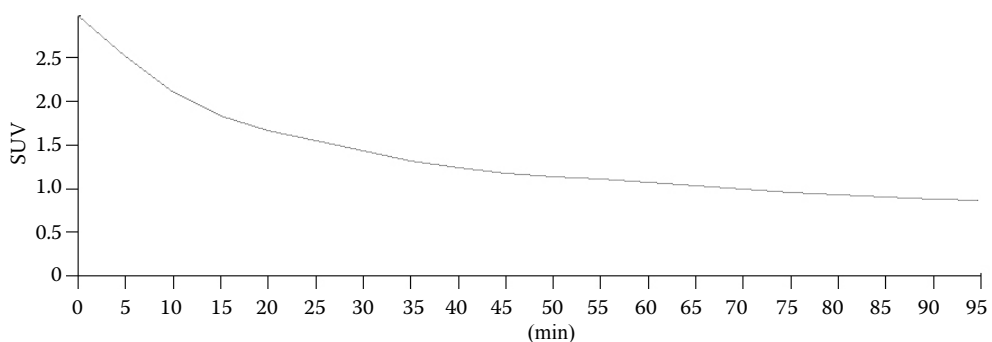

Figure 4. The time activity curve of ^{18}F-FDG obtained from the region of interest (ROI) around the liver of a cat
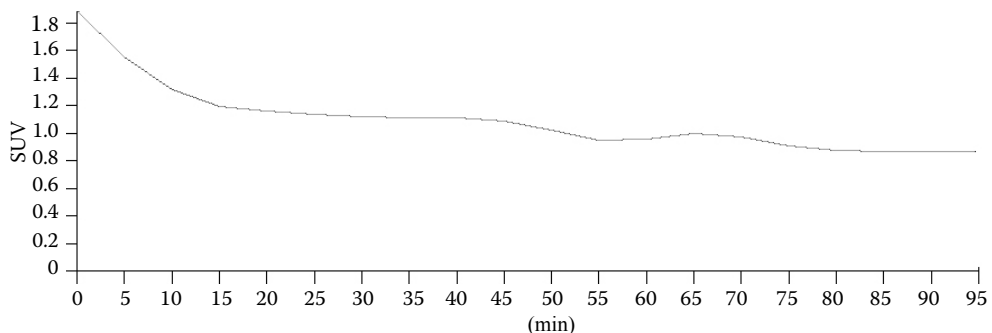

Figure 5. The time activity curve of ^{18}F-FDG obtained from the region of interest (ROI) around the left kidney of a cat
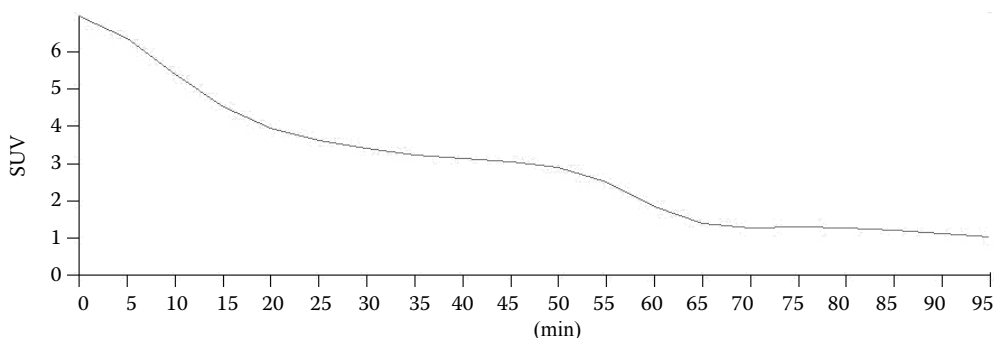
Figure 6. The time activity curve of ^{18}F-FDG obtained from the region of interest (ROI) around right kidney of a cat
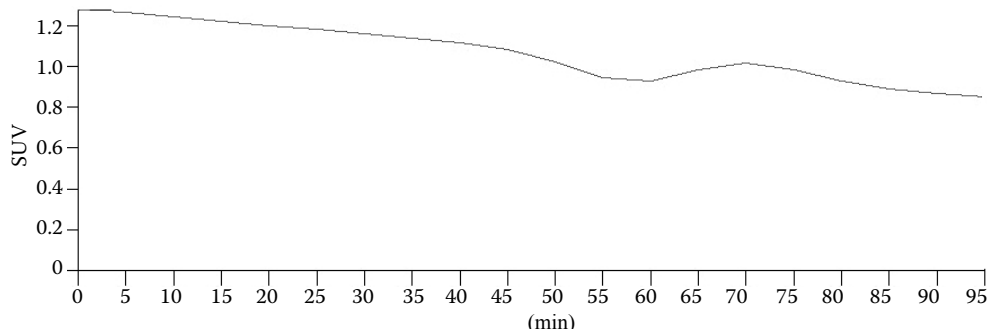

Figure 7. The time activity curve of ^{18}F-FDG obtained from the region of interest (ROI) around the spleen of a cat

0.28; 60 min SUV 0.82 ± 0.21, 90 min SUV 0.66 ± 0.14) compared to that of other organs (Figure 5).

The SUV of the left ventricular myocyte was relatively lower than that observed in tissues from other organs. In the case of the left ventricular myocytes, the SUV showed a gradual increase in two of the five cats.

Our results regarding ^{18}F-FDG uptake in cat myocytes were mixed. In two animals, the accumulation of ^{18}F-FDG in the left ventricular myocytes showed a gradual decrease with time; however, in one animal, the SUV increased from 1.53 at 0 min to 3.5 at 90 min, while in another animal the value increased from 1.8 at 0 min to 2.2 at 90 min. In the remaining animal, there was an insignificant increase in SUV from 1.6 to 1.68 (Figure 6).

The results regarding the SUV of ^{18}F-FDG in the left blood pools of the cat were more consistent. Among all five animals, the SUV decreased with time. Interestingly, in the two animals that showed an increase in ^{18}F-FDG SUV in the ventricular myocytes over time, an insignificant decrease in SUV within the left blood pool was observed (Figure 7).

Our findings show that the percent changes in ^{18}F-FDG SUV of the cat organs over time are as follows: liver 27.3%, from 2.86 to 0.78; spleen-17.9%, from 0.95 to 0.17: right kidney – 32.1%, from 5.27 to 1.69: left kidney – 38.9%, from 4.58 to 1.78. In comparison, the ^{18}F-FDG SUV in dog organs over time is as follows: liver 44%, spleen 90.7%, right kidney 38.6%, left kidney 38.6%.

When observing the change in ^{18}F-FDG SUV from 0 to 90 min, the distribution rate for each organ, our data suggest that the ^{18}F-FDG SUV decrease rate in the feline is greater than in the dog.

DISCUSSION

PET imaging using ^{18}F-FDG is rapidly gaining a critical role in the clinical evaluation of patients with cancer. However, PET images lack anatomical landmarks for topographic orientation, and identification of abnormal glucose metabolic activity in regions close to organs with variable physiological ^{18}F-FDG uptake can be difficult.

To overcome these difficulties, a combined PET/CT scanner that acquires both functional PET and CT images has been recently developed, and its use as a diagnostic tool has increased rapidly. Since PET/CT is a combination of PET for functional information and CT for morphological information, their combination is synergistic.

Generally, most PET imaging data is gained from a static frame. However, dynamic data acquisition is arguably more informative than static images because it provides the tracer distribution in terms of time and space within the ROI.

Therefore, it is important to evaluate the quantitative accuracy regarding list mode or dynamic PET acquisition before use in clinical and study applications. The SUV is a semi-quantitative value that one

can easily access whenever PET/CT is performed under physiological or pathologic circumstances (Lindholm et al. 1993; Hamberg et al. 1994).

The SUV depends on acquisition, reorganisation, reconstitution, and ROI parameters. Thus, obtaining an accurate SUV requires a clean acquisition standard and analysis protocol.

The results from this study showed that the uptake of ^{18}F-FDG in the stomach and small and large intestines was variable and characterised by focal or diffuse uptake of ^{18}F-FDG. These results were similar to results from human and dog studies (Yasuda et al. 1998; Kostakoglu et al. 2004; Rosenbaum et al. 2006). The reason for ^{18}F-FDG uptake into the digestive organs is not known.

Increases in smooth muscle intake, full energetic mucous membrane in metabolism, or intake by colon bacteria are possible reasons for this phenomenon (Abouzied et al. 2005). The lung showed the lowest SUV compared with the other organs, which is consistent with the observation that ^{18}F-FDG does not accumulate in normal lung tissue. However, if lung cancer is present, the SUV will increase due to tumour metabolism (Vansteenkiste et al. 1999; Weber et al. 2000; Lee et al. 2010).

The average SUV for the kidney, liver, and spleen obtained 60 min post-^{18}F-FDG injection into healthy humans was 2.33, 2.17, and 1.65, respectively. The average SUVs for dog kidney, liver, and spleen at 60 min were 2.88, 2.75, and 1.71, respectively.

Thus, data suggest a similar average SUV for humans and canines. In the current study, the average SUVs for cat kidney, liver, and spleen after 60 min were 2.02, 1.00, and 0.24, respectively. The average cat kidney SUV at 60 min was not much different from the SUV of humans or dogs.

Additionally, the 60-min SUV for the right kidney was 2.04 while in the left kidney the value was 2.00, a difference that is not significant. This difference seems to be caused by the use of a more accurate drawing of uncertain borders in a PET image.

It could be considered that the SUV values of liver and spleen are relatively lower than those of humans and dogs, and the SUV values at 0-min, and 60-min for the kidney, liver, and spleen, the kidney's excretion rate of ^{18}F-FDG is higher than those of the liver and spleen.

The cellular distribution of ^{18}F-FDG is largely dependent on two factors: The presence and activity of various glucose transporter proteins (GLUT 1–12) that allow ^{18}F-FDG entry into the cell, and

hexokinase enzyme activity that works to phosphorylate and thus trap ^{18}F-FDG within the cell, thereby preventing its passage through additional steps of glycolysis (Fowler and Ido 2002; Medina and Owen 2002; Wood and Trayhurn 2003).

Mammalian hepatocytes generally contain two enzymes responsible for phosphorylation of glucose to glucose-6-phosphate in the first step of glycolysis: hexokinase and glucokinase (MacDonald et al. 1984). These enzymes may also phosphorylate ^{18}F-FDG to ^{18}F-FDG -6-phosphate. Hexokinase and glucokinase are both present in the canine liver, but the feline liver does not contain appreciable levels of glucokinase activity (Ballard 1965).

In our previous experiments, cat spleens were not studied, (LeBlanc et al. 2009). However, in this study, the spleen ^{18}F-FDG SUV was high at the beginning of the time-course and then gradually decreased. As the accumulation was observed at the outset but decreased after sufficient accumulation, the necessity for dynamic examination is supported; we could verify the SUV of the spleen by establishing an ROI after correctly determining the uncertain border of the organ.

Poor myocardial uptake of ^{18}F-FDG in this study is consistent with typical findings in humans after an 18 h fast. In humans, ^{18}F-FDG intake may not occur in the myocardium due to a change of disposition of this myocardium after an 18–24 h fast. Within the myocardium, the use of glucose is variable, depending on factors such as glucose serum level and insulin levels, what the myocardium energy disposition at empty stomach is superior as fatty acid (Nuutinen et al. 1999).

The fast is an significant factor in this analysis as anaesthesia is an important tool in veterinary science. As glucose is competing with ^{18}F-FDG the drop in blood glucose levels due to fasting is important because it increases ^{18}F-FDG intake by malignant tumour tissues and tissues affected by hypermetabolic disease. In a previous experiment, animals were fasted for 12–18 h before examination. Sixty minutes after initiation of the experiment, the average SUV of heart tissue was 3.58 in the transverse scan and 3.34 in the sagittal scan (LeBlanc et al. 2009). In the current study, the animals were fasted for 24 h before examination.

Sixty minutes after examination, the average SUV of the heart was 1.46. In addition, we measured the change of activity in the blood by obtaining the dynamic SUV of the blood pool. We posit that the SUV decreased due to the prolonged duration of an

empty stomach. In this experiment and also in our previous findings, the left myocardial activity was highly variable. However, only the static data was obtained in the previous experiment; therefore, it is impossible to tell whether the SUV was increasing or decreasing.

In this experiment, two of five cats showed a gradual decrease in SUV with time, while two other animals showed a gradual increase, and one animal showed a faint increase.

These results seem to have resulted from the use of fatty acid as a disposition medium into the myocardium at the time of fasting; however, we could not determine the exact reason in this experiment due to the lack of comparative data. It is known that individual differences can also be present within study subjects (Engel et al. 1996; Gordon et al., 1997; Ramos et al. 2001; Tan and Ong 2004).

Differently from a person who fasts just 6 hours before the inspection, in the case of a cat which must be put under anaesthesia, and fast for 24 h before the time of inspection, for the change of various individuals of left ventricular myocyte regarding glucose intake of myocardium, the study on fatty acid use as disposition in myocardium not yet known when cat fasts will have to proceed more (Crippa et al. 1997; Lee et al. 2005).

The left blood pools of all five cats showed an SUV decrease by 90 min. Interestingly, a faint increase was observed in the SUV of the left blood pool in the two animals in which the SUV of the ventricular myocytes increased. In the future, the correlation between ventricular myocyte and blood pool SUV should be studied.

Data from canine experiments shows that the SUV decrease by at least 50% when comparing the 0 to 90 min results for both kidneys and the liver. Our data show that the feline 90-min SUVs from those same organs were decreased to less than half the values observed at 0 min. Therefore, both dog and cat SUV values for kidneys and liver decrease by at least 50% by 90 min.

Additionally, the dog SUV in liver and kidneys plateaus at 60-min, followed by a steady decrease in ^{18}F-FDG (LeBlanc et al. 2008). The results from cats show a sudden decrease in ^{18}F-FDG at 60 min. The SUVs of the dog's kidneys are higher (right 6.70, left 6.24) at 0 min, compared to those of the other organs (liver 5.75, spleen 1.73, left blood pool 4.35, left ventricular myocyte 3.12), Our data also showed a higher SUV for the cat kidneys (right kidney 5.27, left kidney 4.58) than the other organs

(liver 2.86, spleen 1.54, left blood pool 3.61, left ventricular myocyte 1.64).

Thus, cats and dogs share another trait regarding SUVs in thoracoabdominal organs.

In contrast, the discharge rate of ^{18}F-FDG for each organ of the cat studied was quite different from that observed for dogs.

The cat discharge rates are as follows: liver 27.3%, spleen 17.9 %, right kidney 32.1%, left kidney 38%. The dog discharge rate for the liver is 44%, for the spleen it is 90.7%, for the right kidney 38.6%, and for the left kidney the value is 38.6%. Thus, the discharge speed of ^{18}F-FDG from the cat liver and spleen was relatively fast.

There are a few limitations to this study. First, the sample size was small. Second, the animals were anaesthetised with an injectable anaesthetic. In a similar study performed with rats, Xy/Ke anaesthesia increased the blood ^{18}F-FDG as it disrupted the insulin discharged by a rat which was fasted for 4 h thus decreasing the tumour intake ratio. On the other hand, pentobarbital use resulted in a similar, but less severe response in insulin resistance. In a tumour model study on rats, isoflurane anaesthesia did not have any influence on a xenograft tumour (Fueger et al. 2006).

The use of general anaesthesia shows falsely low ^{18}F-FDG intake in most organs due to changes in the immanent metabolism path. The effect of general anaesthesia on dog or cat ^{18}F-FDG intake has not been explored.

To minimise the diversity of ^{18}F-FDG intake, the use of a single protocol for general anaesthesia should be recommended. The third caveat to our study is that only mature cats were included in this experiment. This is significant because the ratio of brown fat which consumes a large number of calories is greater in young animals than in adults. Brown fat is diverse in its degree and distribution of ^{18}F-FDG intake. As in dual-time-point scanning and malignant tumours, the hypermetabolic brown fat usually showed a significant ^{18}F-FDG increase. This brown fat is an important cause of false positive results. As previously mentioned, young cats were not included in this experiment. However, studies to compare the ^{18}F-FDG intake rate per organ in young cats vs. that in old cats based on the presence of brown fat should be conducted in the future.

Given the lack of information regarding cat ^{18}F-FDG intake ratios, the basic information obtained in this work is helpful despite the mentioned

limitations. The use of PET/CT is expected to increase in numerous fields, including physiology, pathology, and oncology.

The normal cat SUV data of major organs described here could be used in cat PET/CT studies and in the clinical evaluation of various cat diseases. Furthermore, PET/CT can provide higher quality images over shorter examination times than conventional PET.

REFERENCES

Abouzied MM, Crawford ES, Nabi HA (2005): ^{18}F-FDG imaging: pitfalls and artifacts. Journal of Nuclear Medicine Technology 33, 145–155.

Ballard FJ (1965): Glucose utilization in the mammalian liver. Comparative Biochemistry and Physiology 14, 437–443.

Crippa F, Gavazzi C, Bozzetti F, Chiesa C, Pascali C, Bogni A, De Sanctis V, Decise D, Schiavini M, Cucchetti G, Bombardieri E (1997): The influence of blood glucose levels on [^{18}F]fluorodeoxyglucose (FDG) uptake in cancer: a PET study in liver metastases from colorectal carcinomas. Tumori 83, 748–752.

Engel H, Steinert H, Buck A, Berthold T, Huch Boni RA, von Schulthess GK (1996): Whole-body PET: physiological and artifactual fluorodeoxyglucose accumulations. Journal of Nuclear Medicine 37, 441–446.

Fueger BJ, Czernin J, Hildebrandt I, Tran C, Halpern BS, Stout D, Phelps ME, Weber WA (2006): Impact of animal handling on the results of ^{18}F-FDG PET studies in mice. Journal of Nuclear Medicine 47, 999–1006.

Fowler JS, Ido T (2002): Initial and subsequent approach for the synthesis of ^{18}F-FDG. Seminars Nuclear Medicine 32, 6–12.

Gordon BA, Flanagan FL, Dehdashti F (1997): Wholebody positron emission tomography: normal variations, pitfalls, and technical considerations. American Journal of Roentgenology 169, 1675–1680.

Gorospe SL, Echeveste AJ, Raman S (2006): Positron-emission tomography/computed tomography: artifacts and pitfalls in cancer patients. Journal of Radiology 48, 189–204.

Hamberg LM, Hunter GJ, Alpert NM, Choi NC, Babich JW, Fischman AJ (1994): The dose uptake ratio as an index of glucose metabolism: useful parameter or oversimplification? Journal of Nuclear Medicine 35, 1308–1312.

Kostakoglu L, Hardoff R, Mirtcheva R, Goldsmith SJ (2004): PET/CT fusion imaging in differentiating physiologic from pathologic FDG uptake. RadioGraphics 24, 1411–1431.

LeBlanc AK, Jakoby B, Townsend DW, Daniel GB (2008): Thoracic and abdominal organ uptake of 2-deoxy-2-[^{18}F] fluoro-D-glucose (^{18}F-FDG) with positron emission tomography in the normal dog. Veterinary Radiology and Ultrasound 49, 182–188.

LeBlanc AK, Wall JS, Morandi F, Kennel SJ, Stuckey A, Jakoby B, Townsend DW, Daniel GB (2009): Normal thoracic and abdominal distribution of 2-deoxy-2-[^{18}F] fluoro-D-glucose (^{18}F-FDG) in adult cats. Veterinary Radiology and Ultrasound 50, 436–441.

Lee KH, Ko BH, Paik JY, Jung KH, Choe YS, Choi Y, Kim BT (2005): Effects of anesthetic agents and fasting duration on ^{18}F-FDG biodistribution and insulin levels in tumor-bearing mice. Journal of Nuclear Medicine 46, 1531–1536.

Lee MS, Lee AR, Jung MA, Lee IH, Choi JH, Chung HW, Jeong SW, Nahm SS, Eom KD (2010): Charicterization of physiologic ^{18}F-FDG uptake with PET-CT in dogs. Veterinary Radiology and Ultrasound 51, 670–673.

Lindholm P, Minn H, Leskinen Kallio S, Bergman J, Ruotsalainen U, Joensuu H (1993): Influence of the blood glucose concentration on FDG uptake in cancer. Journal of Nuclear Medicine 34, 1–6.

Liu X, Comtat C, Michel C, Kinahan P, Defrise M, Townsend D (2001): Comparison of 3-D reconstruction with 3D-OSEM and with FORE + OSEM for PET. IEEE Transactions on Medical Imaging 20, 804-814.

Macapinlac HA (2008): Clinical applications of positron emission tomography/computed tomography treatment planning. Seminars Nuclear Medicine 38, 137-140.

MacDonald ML, Rogers QR, Morris JG (1984): Nutrition of the domestic cat, a mammalian carnivore. Annual Review of Nutrition 4, 521–562.

Medina RA, Owen GI (2002): Glucose transporters: expression, regulation and cancer. Biological Research 35, 9–26.

Nuutinen J, Minn H, Bergman J, Haaparanta M, Ruotasalainen U, Laine H, Knuuti J (1999): Uncoupling of fatty acid and glucose metabolism in malignant lymphoma: a PET study. British Journal of Cancer 80, 513–518.

Ramos CD, Erdi YE, Gonen M, Riedel E, Yeung HW, Macapinlac HA, Chisin R, Larson SM (2001): FDG-PET standardized uptake values in normal anatomical structures using iterative reconstruction segmented attenuation correction and filtered back-projection. European Journal of Nuclear Medicine 28, 155–164.

Rosenbaum SJ, Lind T, Antoch G, Bockisch A (2006): False-positive FDG PET uptake-the role of PET/CT. European Radiology 16, 1054–1065.

Tan LT, Ong KL (2004): Semi-quantitative measurements of normal organs with variable metabolic activity FDG

PET imaging. Annals of the Academy of Medicine Singapore 33, 183–185.

Tsukamoto E, Ochi S (2006): PET/CT today: system and its impact on cancer diagnosis. Annals of Nuclear Medicine 20, 255–267.

Vansteenkiste JF, Stroobants SG, Dupont PJ, De Leyn PR, Verbeken EK, Deneffe GJ, Mortelmans LA, Demedts MG (1999): Prognostic importance of the standardized uptake value on ^{18}F-fluoro-2-deoxy-glucosepositron emission tomography scan in non-small-cell lung cancer: an analysis of 125 cases. Journal of Clinical Oncology 17, 3201–3206.

Visser EP, Philippens ME, Kienhorst L, Kaanders JH, Corstens FH, de Geus-Oei LF, Oyen WJ (2008): Comparison of tumor volumes derived from glucose met-

abolic rate maps and SUV maps in dynamic ^{18}F-FDG PET. Journal of Nuclear Medicine 49, 892–898.

Weber WA, Schwaiger M, Avril N (2000): Quantitative assessment of tumor metabolism using FDG-PET imaging. Nuclear Medicine and Biology 27, 683–687.

Wood IS, Trayhurn P (2003): Glucose transporters (GLUT and SGLT): expanded families of sugar transport proteins. British Journal of Nutrition 89, 3–9.

Yasuda S, Takahashi W, Takagi S, Fujji H, Ide M, Shohtsu A (1998): Factors influencing physiological FDG uptake in the intestine. Tokai Journal of Experimental and Clinical Medicine 23, 241–244.

Corresponding Author:

K.C. Lee, College of Veterinary Medicine, Chonbuk National University, Jeonju 561-756, Korea
Tel. +82 63 270 2558, E-mail: kclee@chonbuk.ac.kr